FREQUENCY OFFSET AND TIMING ESTIMATION IN SLOWLY-VARYING FADING CHANNELS: A CYCLOSTATIONARY APPROACH

[1] *Fulvio Gini* and [2] *Georgios B. Giannakis*

[1]Dept. "Ingr. dell' Informazione", Univ. of Pisa, via Diotisalvi, 2 I-56126 Pisa, ITALY
Tel: (+39) 50-568550 Fax: (+39) 50-568522 E-mail: gini@iet.unipi.it
[2]Dept. of Electrical Engr., Univ. of Virginia, Charlottesville, VA 22903-2442, U.S.A.
Tel: (804) 924-3659 Fax: (804) 924-8818 E-mail: georgios@virginia.edu

ABSTRACT

Two open-loop algorithms are developed for estimating jointly frequency offset and symbol timing of a linearly modulated waveform transmitted over a frequency-flat fading channel. The methods exploit the received signal's cyclostationarity, and with respect to existing solutions they: (i)take into account the presence of time-selective fading effects; (ii)do not need training data; (iii)do not rely on the Gaussian assumption of the complex equivalent low-pass channel process, and (iv)are tolerant to additive stationary noise of any color or distribution. Performance analysis using Monte Carlo simulations, unifications, and comparisons with existing approaches are also reported.

1. INTRODUCTION AND MODELING

Mis-timing and frequency drifts arise in digital communication systems due to propagation, Doppler effects, and mismatch between transmit and receive oscillators. Adaptive feedback loops are popular for tracking, but in order to avoid "hang-up" effects encountered with bursty transmissions, feedforward batch estimators based on the preamble (training data) are also needed for acquisition [4], [6]. With fading effects, present in cellular terrestrial radio and ionospheric channels, synchronization problems are even more challenging [8]. Non data-aided, open-loop algorithms were proposed in [10] and [5], and their performance was simulated for time- and frequency-selective fading; however, the analysis assumed constant fading over the entire burst.

This paper relies on cyclostationary statistics of fractionally sampled data to develop fully digital non data-aided frequency offset and symbol timing estimation algorithms for linearly modulated waveforms transmitted over frequency-flat fading channels. Cyclostationarity was also used in [9], but fading effects were not considered. Even if not clearly acknowledged, cyclostationarity has been exploited for synchronization purposes also in [7], [5], and [3]. The underlying common idea is to use nonlinear combinations of delayed versions of the data to reveal periodic components containing synchronization parameters. In this paper, we attempt to unify and improve upon these approaches within a discrete-time cyclostationary framework.

Consider linear modulation and transmission over a frequency-flat fading channel. The complex envelope of the received signal is (e.g., [8, Ch. 14], [10]):

$$r_c(t) = \mu_c(t)e^{j2\pi f_e t}\sum_l w(l)g_c^{(tr)}(t-\epsilon T - lT) + n_c(t) \quad (1)$$

where $\mu_c(t)$ is the fading-induced multiplicative noise, $g_c^{(tr)}(t)$ is the transmitter's signaling pulse, T is the symbol period, $w(l)$'s are the complex information symbols, f_e is the frequency offset, and ϵT is the propagation delay within a symbol period ($0 \le \epsilon < 1$); noise $n_c(t)$ is stationary but not necessarily white and/or Gaussian (subscript c denotes continuous-time signals).

Let $g_c^{(rec)}(t)$ be the matched filter (MF) at the receiver and let $*$ denote convolution. The MF output, $x_c(t) := r_c * g_c^{(rec)}(t)$, is (over)sampled at a rate P/T to yield the discrete-time data:

$$x(n) = \mu(n)\, e^{j\frac{2\pi}{P}f_e T n}\sum_l w(l)g(n-lP) + v(n)\,, \quad (2)$$

with $x(n) := x_c(t)|_{t=nT/P}$, $\mu(n) := \mu_c(t)|_{t=nT/P}$, $v(n) := n_c * g_c^{(rec)}(t)|_{t=nT/P}$, and $g(n) := g_c(t-\epsilon T)|_{t=nT/P}$, where $g_c(t) := g_c^{(tr)} * g_c^{(rec)}(t)$.

Models (1) and (2) are valid as far as:
(i)$\mu_c(t)$ is approximately constant over a pulse; i.e., the Doppler spread $B_\mu T$ is small [8, Ch. 14], where B_μ denotes the bandwidth of $\mu_c(t)$. For practical systems $B_\mu T = 10^{-3}$ corresponds to very slow fading while rapidly fading channels have $B_\mu T = 10^{-1}$;
(ii) f_e is small compared to $1/T$ (see also [4], [5], [10]).

With regards to (2) we also assume that:
(as1)$w(n)$ is zero-mean, iid from a finite-alphabet, complex constellation, with variance σ_w^2;
(as2)$\mu(n)$ is stationary complex process with autocorrelation $m_{2\mu}(\tau) := E\{\mu(n)\mu^*(n+\tau)\}$;
(as3)$v(n)$ is a wss complex process, independent of $\mu(n)$; both $v(n)$ and $\mu(n)$ are mixing with absolutely summable cumulants – a condition satisfied by all finite memory signals in practice.

Our objective is to estimate f_e and ϵ in (1) based on N consecutive samples $\{x(n);\ n = 0, 1, \ldots, N-1\}$ from (2), corresponding to N/P transmitted symbols.

If $w(n)$ is given (data-aided scenario), and the distributions of $\mu(n)$ and $v(n)$ are known (e.g., $v(n)$ is Gaussian, or, iid non-Gaussian with known parameters), then maximum likelihood (ML) estimation of f_e and ϵ is possible

0-7803-3944-4/97/$10.00

although computationally demanding. We seek consistent, albeit computationally efficient estimates, that can not only initialize the nonlinear search required by ML estimates in the data-aided case, but most importantly remain operational in the blind (non-data-aided) scenario with realistic fading and colored noise processes of unknown distributions.

2. CYCLOSTATIONARY APPROACH

Under (as1)-(as3), the correlation $m_{2x}(n;\tau) := E\{x(n)\, x^*(n+\tau)\}$ of $x(n)$ in (2) is:

$$m_{2x}(n;\tau) = \sigma_w^2 m_{2\mu}(\tau)\, e^{-j\frac{2\pi}{P}f_eT\tau} \sum_l g(n-lP) \times g^*(n+\tau-lP) + m_{2v}(\tau)\ . \quad (3)$$

For a fixed τ, $m_{2x}(n;\tau)$ is periodic (in n) with period P and Fourier Series coefficients (termed cyclic correlations) $\mathcal{M}_{2x}(k;\tau) := (1/P)\ \sum_{n=0}^{P-1}\ m_{2x}(n;\tau)\exp(-j\frac{2\pi}{P}kn)$ at cycles $2\pi k/P$ with $k = -P/2, \ldots, P/2-1$ for P even.

We wish to reveal the dependence of $\mathcal{M}_{2x}(k;\tau)$ on ϵT. Suppose P is chosen to satisfy $P > 2TB_g$, where B_g is the bandwidth of $g_c(t)$; thus, sampling at a rate $T_s^{-1} := P/T$ does not introduce aliasing and hence, $G(f) := \sum_n g(n)\exp(-j2\pi fn) = (1/T_s)G_c(f/T_s)\exp(-j2\pi f\epsilon)$, for $|f| \leq 1/2$. Evaluating Fourier Series and applying Parseval's relation in (3) will therefore yield:

$$\mathcal{M}_{2x}(k;\tau) = \frac{\sigma_w^2}{P}\, m_{2\mu}(\tau)\, e^{-j\frac{2\pi}{P}f_eT\tau}\, e^{-j2\pi k\epsilon}\, G_2(k;\tau) + m_{2v}(\tau)\delta(k)\ , \quad (4)$$

where $G_2(k;\tau) := (P/T)\int_{-P/(2T)}^{P/(2T)} G_c^*(\beta - k/T)G_c(\beta)\exp(-j2\pi\beta\tau T/P)d\beta$.

We infer from (4), that frequency offset and symbol timing appear (and can be estimated) as separable 1-D complex exponentials in the 2-D sequence $\mathcal{M}_{2x}(k;\tau)$: f_e w.r.t. the lag τ and ϵ w.r.t. the cycle k.

Because $G_2(k;\tau)$ is known, we can define for $(k;\tau) \in \mathcal{I}_{G2} := \{(k;\tau)|\ G_2(k;\tau) \neq 0\}$ the "pulse-compensated" cyclic correlation $\mathcal{M}_2(k;\tau) := G_2^{-1}(k;\tau)\mathcal{M}_{2x}(k;\tau)$ from which f_e and ϵ can be retrieved via:

$$f_e = -\frac{P}{4\pi T\tau}\ \arg\{\mathcal{M}_2(k;\tau)\mathcal{M}_2(-k;\tau)\},\quad k>0 \quad (5)$$

$$\epsilon = -\frac{1}{2\pi k}\arg\{\mathcal{M}_2(k;\tau)e^{j\frac{2\pi}{P}f_eT\tau}\}\ , \qquad k\neq 0\ . \quad (6)$$

In (5), $\tau \in [1, L_\tau]$ while in (6), $\tau \in [0, L_\tau]$, where L_τ denotes the maximum τ in $\mathcal{I}_{G2}$. By avoiding the cycle $k = 0$, noise $v(n)$ can be avoided with ensembles. However, in practice noise affects $\mathcal{M}_{2x}(k;\tau)$ which is estimated using the (normalized) FFT of the product $x(n)x^*(n+\tau)$:

$$\hat{\mathcal{M}}_{2x}(k;\tau) := \frac{1}{N}\sum_{n=0}^{N-1} x(n)x^*(n+\tau)e^{-j\frac{2\pi}{P}kn}\ . \quad (7)$$

Under (as3), $\hat{\mathcal{M}}_{2x}$ is asymptotically unbiased and mean square sense consistent [2]; hence, the estimators of f_e and ϵ, in (5) and (6) are also consistent.

Estimating f_e and ϵ based on (5) and (6) may require phase unwrapping which motivates working in the cyclic spectral domain. The cyclic spectrum of $x(n)$ is defined as $\mathcal{S}_{2x}(k;f) := FT_{\tau\to f}[\mathcal{M}_{2x}(k;\tau)] = \sum_\tau \mathcal{M}_{2x}(k;\tau)\exp(-j2\pi f\tau)$. Similar to (4), its "pulse-compensated" version, $\mathcal{S}_2(k;f) := \mathcal{G}_2^{(-1)} * \mathcal{S}_{2x}(k;f)$, is

$$\mathcal{S}_2(k;f) = \mathcal{S}_{2\mu}(f+\frac{f_e}{P})e^{-j2\pi k\epsilon} + \mathcal{G}_2^{(-1)} * \mathcal{S}_{2v}(f)\delta(k), \quad (8)$$

where $\mathcal{G}_2^{(-1)}(k;f) := FT_{\tau\to f}[G_2^{-1}(k;\tau)]$ and $\mathcal{S}_{2\mu}(f) := FT_{\tau\to f}[m_{2\mu}(\tau)]$. Let us also assume that, [8, Ch. 14], [1]: (as4) $\mu(n)$ is a complex low-pass process with $\mathcal{S}_{2\mu}(f)$ peaking at a known frequency (w.l.o.g. suppose it peaks at $f = 0$).

Under (as4), f_e and ϵ can be recovered respectively from:

$$f_e = -\frac{P}{T}\arg\max_f |\mathcal{S}_2(k;f)|,\quad k\neq 0\ , \quad (9)$$

$$\epsilon = -\frac{1}{2\pi k}\ \arg\{\mathcal{S}_2(k;f_e)\},\quad k\neq 0\ . \quad (10)$$

Ambiguity due to spectral folding does not occur in (9) if $|f_eT| < 0.5$, while (5) requires $|f_eT| < 0.25$.

Sample cyclic spectra are used in (9) and (10) when single record data are available. Consistent estimates can be obtained by windowing $\hat{\mathcal{M}}_{2x}(k;\tau)$ with $W^{(2L_g+1)}(\tau)$ having support $[-L_g, L_g]$, $L_g \leq L_\tau$, and Fourier transforming to obtain:

$$\hat{\mathcal{S}}_{2x}(k;f) = \sum_{\tau=-L_g}^{L_g} W^{(2L_g+1)}(\tau)\hat{\mathcal{M}}_{2x}(k;\tau)e^{-j2\pi f\tau}\ . \quad (11)$$

Alternatively, $\mathcal{S}_{2x}(k;f)$ can be estimated directly from the data, relying upon the cyclic periodogram defined as: $I_{2x}^{(N)}(k;f) := N^{-1}X_N(k/P - f)X_N^*(-f)$, where $X_N(f) := \sum_{n=0}^{N-1} x(n)\exp(-j2\pi fn)$. Under (as3), smoothing $I_{2x}^{(N)}(k;f)$ with an appropriate spectral window $W^{(N)}(f)$, yields the estimate

$$\hat{\mathcal{S}}_{2x}(k;f) := \frac{1}{N}\sum_{i=0}^{N-1} I_{2x}^{(N)}(k;\frac{i}{N})W^{(N)}(f-\frac{i}{N})\ , \quad (12)$$

which is consistent and asymptotically normal with computable variance [2].

3. ESTIMATORS AND COMPARISONS

Multiplicative and additive noise effects can be potentially reduced by averaging (5) and (6), or, (9) and (10) over $(k;\tau) \in \mathcal{I}_g/\{k = 0, -P/2\}$. Single cycle-lag or averaged estimators are valid for arbitrary pulse shapes, but in order to compare them with existing methods, we will next specialize $g_c^{(tr)}(t)$, $g_c^{(rec)}(t)$ (and thus $g_c(t)$) to the commonly used raised cosine pulse:

$$g_{rc}(t) = \frac{\sin(\pi t/T)}{\pi t/T}\ \frac{\cos(\pi\alpha t/T)}{(1-4\alpha^2(t/T)^2)}\ , \quad (13)$$

where α in (13) is the rolloff factor ($0 \leq \alpha \leq 1$). To assure causality, we will also assume that (see also [6] and [10]):

(as5) $g_c(t)$ is a truncated and delayed (by t_0) version of $g_{rc}(t)$; i.e., $g_c(t) = g_{rc}(t-t_0)u(t) \cong g_{rc}(t-t_0)$, where $u(t)$ is the unit step function. Under (as5), pulse compensation does not require normalization. Specifically, it turns out that $G_2(k;\tau)$ and thus $\mathcal{M}_{2x}(k;\tau)$ in (4) are nonzero only for cycles $k=0$, $k=1$, and $k=-1$. To reduce noise effects we exclude $k=0$ and estimate f_e and ϵ using

$$\hat{f}_e = -\frac{P}{4\pi T L_g}\sum_{\tau=1}^{L_g}\frac{1}{\tau}\arg\{\hat{\mathcal{M}}_{2x}(1;\tau)\hat{\mathcal{M}}_{2x}(-1;\tau)\} \quad (14)$$

$$\hat{\epsilon} = -\frac{1}{4\pi(L_g+1)}\sum_{\tau=0}^{L_g}[\arg\{\hat{\mathcal{M}}_{2x}(1;\tau)e^{j\frac{2\pi}{P}(\hat{f}_eT-\frac{1}{2})\tau} \times e^{j\frac{2\pi t_0}{T}}\} - \arg\{\hat{\mathcal{M}}_{2x}(-1;\tau)e^{j\frac{2\pi}{P}(\hat{f}_eT+\frac{1}{2})\tau}e^{-j\frac{2\pi t_0}{T}}\}] \quad (15)$$

where t_0 denotes the known delay of $g_{rc}(t)$.

Similarly, with cyclic spectra we find

$$\hat{f}_e = -\frac{P}{2T}\arg\max_f[|\hat{\mathcal{S}}_{2x}(1;f)| + |\hat{\mathcal{S}}_{2x}(-1;f)|] \quad (16)$$

$$\hat{\epsilon} = -\frac{1}{4\pi}[\arg\{\hat{\mathcal{S}}_{2x}(1;\hat{f}_e)e^{j2\pi\frac{t_0}{T}}\} - \arg\{\hat{\mathcal{S}}_{2x}(-1;\hat{f}_e)e^{-j2\pi\frac{t_0}{T}}\}] . \quad (17)$$

Note that estimators in (14), (15) and (16), (17) are consistent, independent of the color and distribution of the additive noise and the fading distortion.

In comparison, the estimators in [10] are given by

$$\hat{f}_e = -\frac{1}{4\pi T}\arg\{\hat{\mathcal{M}}_{2x}(1;P)\hat{\mathcal{M}}_{2x}(-1;P)\} , \quad (18)$$

$$\hat{\epsilon} = -\frac{1}{2\pi}\arg\{\hat{\mathcal{M}}_{2x}(1;\tau)e^{j\frac{2\pi}{P}(\hat{f}_eT-\frac{1}{2})\tau}e^{j\frac{2\pi t_0}{T}}\} . \quad (19)$$

Terms $\exp(-j\pi\tau/P)$ and $\exp(j2\pi t_0/T)$ are necessary to compensate for the effects of $g_c(t)$, but were not included in the continuous-time versions of (19) reported in [10].

Next, we compare (14) with the data-aided, open-loop, fading-free $\hat{f}_e$ estimator in [6]. We wish to quantify the performance loss with blind estimation and also assess the potential gain of (14) over [6] when time-selective fading is present. Define the $L/2$ long window $W(\tau) := [12(L-\tau)(L-\tau+1)-3L^2]/2L(L^2-1)$, and denote with $\hat{r}_z(\tau) := (L-\tau)^{-1}\sum_{n=0}^{L-1}z(n)z^*(n+\tau)$ the sample correlation of symbol rate samples. With known preamble and accurate timing information, the estimator in [6] is:

$$\hat{f}_e = \frac{1}{2\pi T}\sum_{\tau=1}^{L/2}W(\tau)\arg\{\hat{r}_z(\tau)\hat{r}_z^*(\tau-1)\} . \quad (20)$$

Because $z(n) = x(nP)$, we have $\hat{r}_z(\tau) = (L/(L-\tau))\hat{\mathcal{M}}_{2x}(0;\tau P)$, and with fractional sampling (20) reduces to:

$$\hat{f}_e = \frac{1}{2\pi T}\sum_{\tau=1}^{L/2}W(\tau)\arg\{\hat{\mathcal{M}}_{2x}(0;\tau P)\hat{\mathcal{M}}_{2x}(0;\tau P-P)\}. \quad (21)$$

Note that both (14) and (21) exploit the phase shift due to f_e, but (14) invokes cycles $k \neq 0$ to gain tolerance to stationary additive noise.

An alternative timing estimator was proposed in [7]. In our notation, it can be expressed as:

$$\hat{\epsilon} = -\frac{1}{2\pi}\arg\{\hat{\mathcal{M}}_{2x}(1;0)\} , \quad (22)$$

revealing that only the $0th$ lag of the cycle $2\pi/P$ ($k=1$) is exploited in [7]. Joint non-data-aided $\hat{f}_e$ and $\hat{\epsilon}$ estimators based on the fourth-order cyclic moment, were also reported in [5] for MSK modulation (see also [3] for CPM). It can be shown that the timing estimator in [5] is

$$\hat{\epsilon} = -\frac{1}{2\pi}\arg\{\hat{\mathcal{M}}_{4x}(1;-P,0,-P)\} , \quad (23)$$

which shows the link of [5] with fourth-order cyclic moments.

These comparisons show that viewing synchronization parameter estimation within the context of cyclic statistics gives access to a wealth of tools useful to understand statistical properties of estimation algorithms and suggests means of improving them; e.g., with moderate increase in computations, the estimator (23) can be improved by incorporating lags different than $\tau_1=\tau_3=-P$ and $\tau_2=0$, or, by looking at cycles other than $k=1$.

If one is willing to trade-off more computations for optimality, nonlinear (weighted) least-squares matching criteria can be pursued; e.g., using (4) and (7), the estimator of $\theta := (f_e, \epsilon)$ given by

$$\hat{\theta} = \arg\min_{\theta}\sum_{k=1}^{P-1}\sum_{\tau=0}^{L_g}|\hat{\mathcal{M}}_{2x}(k;\tau) - \mathcal{M}_{2x}(k;\tau;\theta)|^2 , \quad (24)$$

does not require phase unwrapping, avoids $v(n)$ by excluding $k=0$, and can be easily augmented to $\tilde{\theta} := (\theta, \theta_\mu)$ in order to estimate jointly models of $\mu(n)$ with parameters θ_μ. The linear approaches of this paper offer reliable initial estimates which are critical to speed up the iterative search required in (24) and prevent convergence to local minima. Even if computationally complex, $\tilde{\theta}$ deserves further research especially in the blind setup where benchmark ML approaches are not applicable.

4. SIMULATIONS

We generated 4-QAM iid symbols with $\sigma_w^2=2$, and pulse shaped them using g_{rc} of (13) truncated to $7P+1$ taps, delayed by $t_0 = 7T/2$, and with $\alpha = 0.5$. A Rayleigh channel (Clarke's model) was simulated as an AR(5) low pass complex circular Gaussian $\mu(n)$ with $\sigma_\mu^2 = 1$. 400 Monte Carlo runs were averaged in Examples 1, 2, 4 and 200 in Example 3.

Example 1 - Frequency offset (14) vs (18): $N/P = 256$ symbols were used with oversampling factor $P=8$, $B_\mu T = 0.05$ (fast fading), $L_g = 16$, and $\epsilon = 0.375$. Figs. 1a and 1b depict bias and mse of $\hat{f}_e$ in (14) and (18) normalized to the symbol rate for $f_eT = 0, 0.1, 0.2$ (solid, dashed, and dash-dotted for (14), and circles, x-marks, stars for (18) respectively). Especially for low SNR, (14) outperforms (18).

Example 2 - Timing (15) vs (19): From the simulations of Example 1, Figs. 2a and 2b show mse of $\hat{\epsilon}$ and $\hat{f}_eT$, vs SNR for $\epsilon = 0.5$, $f_eT = 0.1$, and different Doppler spread values:

$B_\mu T = 0.001$ (very slow fading), $B_\mu T = 0.01$ (slow fading) and $B_\mu T = 0.05$ (fast fading). Especially the performance of $\hat{\epsilon}$ is considerably improved and justifies the extra computations involved in (15) relative to (19) used in [10].

Example 3 - Training vs Blind: We used $N/P = 128$, $P = 8$, $\alpha = 0.5$, $\epsilon = 0.5$. Fig. 3 shows that (16) comes close in terms of bias and mse to the performance of (20) with known, zero-mean, preamble and no fading for $f_eT = 0, 0.1, 0.2$ (solid, dashed, dashdotted for (16), and circles, x-marks, stars for (20)). With the same f_eT values and line types, Fig. 4 illustrates the advantage of (16) over (20) when fading is present ($B_\mu T = 0.05$), even if (20) of [6] requires accurate timing estimates.

Example 4 - Cyclic correlation vs. spectra: Here we compare f_e estimators (14) vs (16). If N is small, then $\hat{\mathcal{M}}_{2x}(k;\tau)$ or $I_{2x}^{(N)}(k;f)$ should be zero-padded to sufficiently large N_{zp} prior to the FFT, so that the bins $\{f_i = i/N_{zp}\}_{i=0}^{N_{zp}-1}$ in (16) are fine enough to allow accurate estimation of f_e. We used $N/P = 128$, $P = 8$, $\alpha = 0.5$, $\epsilon = 0.5$, $L_g = 16$, $N_{zp} = 10^{17}$, $B_\mu T = 0.05$. Fig. 5 shows that with known preamble and in the presence of fading (16) outperforms (14) and hence cyclic spectra are to be preferred.

REFERENCES

[1] W. C. Dam and D. P. Taylor, "An adaptive maximum-likelihood receiver for correlated Rayleigh-fading channel," *IEEE Trans. on Com.*, pp. 2684-2692, 1994.

[2] A. V. Dandawate and G. B. Giannakis, "Asymptotic theory of mixed time averages and kth-order cyclic-moment and cumulant statistics," *IEEE Trans. on Info. Theory*, pp. 216-232, 1995.

[3] A. N. D'Andrea, U. Mengali and M. Morelli, "Symbol timing estimation with CPM modulation," *IEEE Trans. on Commun.*, pp. 1362-1371, 1996.

[4] M. Luise and R. Reggiannini, "Carrier recovery in all-digital modems for burst-mode transmissions," *IEEE Trans. on Com.*, pp. 1169-1178, 1995.

[5] R. Mehlan, Y. Chen and H. Meyr, "A fully digital feedforward MSK demodulator with joint frequency offset and symbol timing estimation for burst mode mobile radio," *IEEE Trans. on Veh. Tech.*, pp. 434-443, 1993.

[6] U. Mengali and M. Morelli, "Data-aided frequency estimation for burst digital transmission," *IEEE Trans. on Com.*, Jan. 1997 (to appear).

[7] M. Oerder and H. Meyr, "Digital filter and square timing recovery," *IEEE Trans. on Commun.*, pp. 605-611, 1988.

[8] J. G. Proakis, *Digital Communications*, third edition, McGraw Hill, Inc., 1995.

[9] J. Riba and G. Vazquez, "Bayesian recursive estimation of frequency and timing exploiting the cyclostationarity property," *Signal Processing*, pp. 21-37, 1994.

[10] K. E. Scott and E. B. Olasz, "Simultaneous clock phase and frequency offset estimation," *IEEE Trans. on Com.*, pp. 2263-2270, 1995.

Acknowledgements: The authors would like to thank Prof. Umberto Mengali for the feedback and the pre-print [6] that he provided. The work in this paper was supported by ONR Grant No. N00014-93-1-0485.

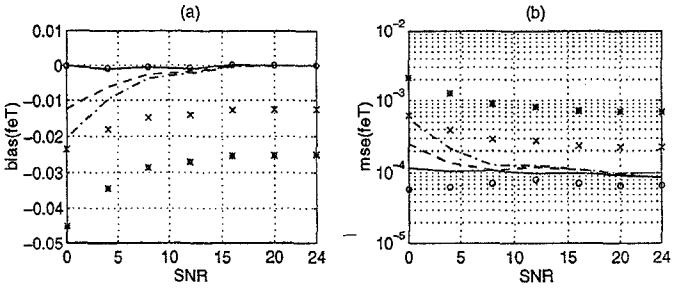

Figure 1. (14) vs (18) $\hat{f}_e$ estimators

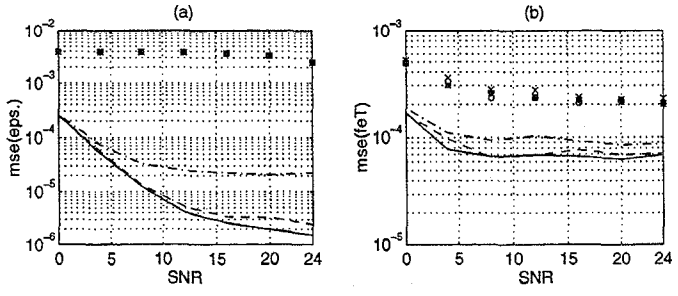

Figure 2. Variable Doppler: (15) vs (19)

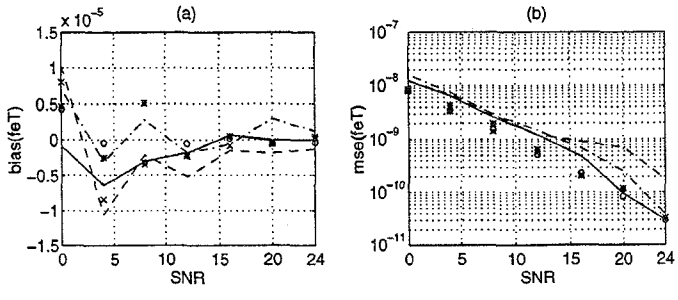

Figure 3. (16) vs (20) $\hat{f}_e$ with known preamble

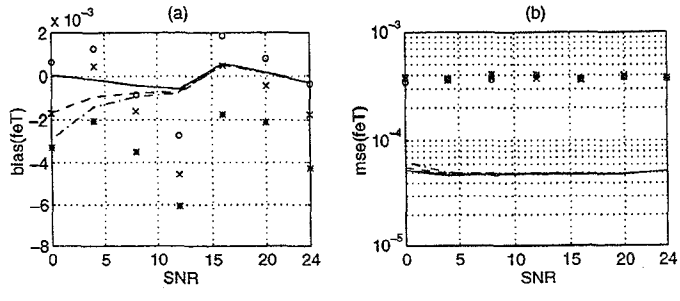

Figure 4. (16) vs (20) $\hat{f}_e$ with fading

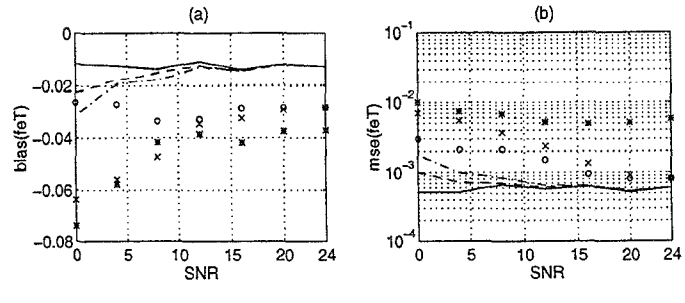

Figure 5. (14) vs (16) with fading